Denoising Method of the Φ-OTDR System Based on EMD-PCC

Wei Chen, Xiaohui Ma, Qinglin Ma, and Jiajie Wen

***Abstract*—To filter out the phase noise of the Φ-OTDR system, a method based on empirical mode decomposition and Pearson correlation coefficient fusion (EMD-PCC) is proposed. First, the EMD-PCC method is simulated. The experimental results show that the SNR increases from 7.32 dB to 13.68 dB. Second, the beat signal detected by the Φ-OTDR system is demodulated by the I/Q quadrature demodulation method. Finally, the phase signal is decomposed by empirical mode decomposition to obtain the modal function and residual component. The Pearson correlation coefficient with the phase signal is calculated. Then, the threshold value is 0.4-1.0. The modal function within the threshold is superimposed with the residual component signal. In this paper, the experimental verification of PZT analog disturbance signal frequencies of 200 Hz, 300 Hz, 400 Hz and 500 Hz is performed. Then, wavelet denoising and EMD-soft denoising are compared with EMD-PCC denoising. Experimental results show that the proposed method can accurately restore the disturbance signal. The experiment of sawtooth disturbance signal frequencies of 400 Hz and 500 Hz verifies the applicability of the algorithm and shows that the method is suitable for other arbitrary forms of disturbance signals. The Φ-OTDR system has an important application in the field of oil and gas exploration. This method provides a good theoretical basis for the exploration field.**

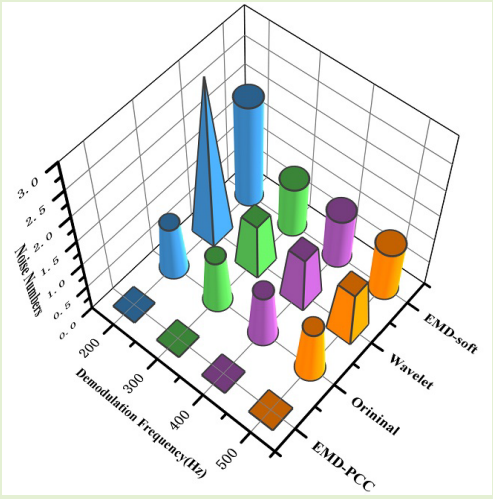

***Index Terms*— Φ-OTDR system, I/Q quadrature demodulation, EMD-PCC.**

I. Introduction

IT IS a common method to obtain formation information by geophones. Distributed optical fiber sensors are an advanced detection method. It has the advantages of flexible deployment, high cost performance and wide measurement range [1]. Compared to traditional methods, this technology realizes large-scale array surveying of seismic wave fields at a lower cost by providing the advantage of improved seismic acquisition [2]. The distributed optical fiber sensing technology (DFOS) is a precise microdeformation detection technology [3], [4] that is widely applied in exploring oil and gas and can monitor the structural health of pipelines in real time [5], [6]. The phase-sensitive optical time domain reflectometer (Φ-OTDR) is an important branch of distributed fiber optic sensors.

When the external disturbance invades the Φ-OTDR system, the vibration signal is wrapped in the phase according to the detection principle of the optical system. By demodulating the phase signal, the intrusion signal can be detected [7], [8]. To solve the problem of phase signal demodulation in Φ-OTDR optical detection systems, there are mainly coherent heterodyne demodulations [9]–[11], 3 × 3 demodulations [12], [13] and phase generation carrier demodulations [14]. In the demodulation of the phase signal, there are many serious problems such as laser frequency drift and accumulated phase noise. Generally, the Φ-OTDR system requires a stable ultranarrow linewidth laser source. However, most commercial lasers do not have a stable frequency and have the problem of low LFD. In addition, accumulated phase noise will be generated when light is transmitted in the sensing fiber, which will affect the demodulation result of the phase signal [15]. Therefore, eliminating noise signals has become a critical step.

In recent years, researchers have proposed many methods to improve phase noise, such as the moving average method [9], continuous wavelet transform [16], [17], time signal separation

Manuscript received September 15, 2020; revised October 15, 2020; accepted October 15, 2020. Date of publication October 26, 2020; date of current version April 16, 2021. This work was supported by the Education Department of Jilin Province under Grant JJKH20190544KJ. The associate editor coordinating the review of this article and approving it for publication was Prof. Carlos Marques. *(Corresponding author: Xiaohui Ma.)*

Wei Chen is with the School of Photoelectric Engineering, Changchun University of Science and Technology (CUST), Changchun 130022, China, and also with the Changchun Institute of Optics, Fine Mechanics and Physics (CIOMP), Chinese Academy of Sciences, Changchun 130033, China (e-mail: chenw2001@126.com).

Xiaohui Ma, Qinglin Ma, and Jiajie Wen are with the School of Photoelectric Engineering, Changchun University of Science and Technology (CUST), Changchun 130022, China (e-mail: mxh@cust.edu.cn; 1721868813@qq.com; wenjiajie9504@163.com).

Digital Object Identifier 10.1109/JSEN.2020.3033674

and determination algorithm [18], differential phase method and adaptive two-dimensional bilateral filtering method [19]. With the rapid development of wavelet theory, it has been introduced into denoising methods. After Liu *et al.* used adaptive wavelet threshold denoising, the dynamic range of backscattered power increased by 3.72 dB, 3.43 dB and 3.37 dB [20]. Qin *et al.* used the wavelet contraction method, so that the distributed vibration measurement of 20 Hz and 8 kHz events can be detected with a 5 ns light pulse at a sensing length of 1 km. In modern signal processing, the compressed sensing theory is introduced. Qu *et al.* introduced compressed sensing into the Φ-OTDR system, and the experimental results showed that the SNR increased to 34.39 dB [21], [22].

However, because the demodulated phase signal of the Φ-OTDR system is nonlinear and nonstationary, this method may not make significant progress. Empirical mode decomposition (EMD) has a good effect in the analysis of nonlinear and nonstationary signals. The prominent feature of EMD is the decomposition method based on the original data, which makes the EMD method adaptive [23], [24]. Therefore, the EMD method is applied to sensor signal processing in many fields such as water waves, biomedical engineering, time series analysis and damage detection [25]. Recently, EMD technology has been introduced into Φ-OTDR system denoising. Qin *et al.* applied EMD to a Φ-OTDR system. When the frequency is 100 Hz and 1.2 kHz, the signal-to-noise ratio improves to 42.52 dB and 39.58 dB, respectively [26]. He *et al.* proposed a clear iterative EMD interval threshold (EMD-CIIT) method, and the SNR increased from 13.3 dB and 13.63 dB to 30.9 dB and 32.82 dB, respectively [27]. Li *et al.* applied the extreme mean complementary empirical mode decomposition (ECEMD) method to the Φ-OTDR system, and the SNR improved by several times. However, when applying the EMD denoising method, the fundamental frequency signal is not always a valid signal. Therefore, the existing method has certain problems.

Through the research and analysis of the demodulated phase signal of the DAS system, a method based on empirical mode decomposition and Pearson correlation coefficient fusion (EMD-PCC) is proposed. To verify the effectiveness of the algorithm, a simulation experiment is designed in this paper; as a result, the SNR increases from 7.32 dB to 13.68 dB. In this paper, a Φ-OTDR system is built. The beat frequency signal detected by the optical system is demodulated to obtain the phase signal. The phase signal undergoes EMD decomposition to obtain the IMF and RES. Then, one must calculate the Pearson correlation coefficient with the phase signal and set the PCC value for the threshold interval to be 0.4-1.0. The IMF and RES signals in the threshold interval are linearly superimposed. In this paper, the experimental verification is performed for the PZT analog disturbance signal frequencies of 200 Hz, 300 Hz, 400 Hz and 500 Hz. Then, wavelet denoising and EMD-soft denoising are compared with EMD-PCC denoising. Experimental results show that the proposed method can accurately restore the disturbance signal. The experiment of sawtooth disturbance signal frequencies of 400 Hz and 500 Hz verify the applicability of the algorithm. The experimental results show that the method is suitable for other arbitrary forms of disturbance signals.

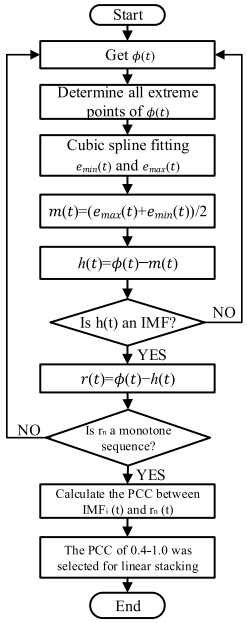

Fig. 1. EMD-PCC flow diagram.

II. EMD-PCC Method

A. Algorithm Principle

In most cases, the signal is nonlinear. When analyzing nonlinear and nonstationary signals, the EMD method has good results. The EMD method can adaptively decompose the signal into the sum of several intrinsic mode functions (IMFs). IMF represents each frequency component in the original signal, and it is arranged from high frequency to low frequency. In addition, the noise signal is superimposed on the IMF signal.

To reduce the effect of the noise signal on the phase signal, Pearson correlation coefficient (PCC) is introduced into the experimental process. PCC is used to measure the degree of linear correlation between two variables, and its value is between -1 and 1. The method is to calculate the PCC values of IMF and RES with the phase signal and select the appropriate threshold for screening. Finally, the obtained signals are linearly superimposed.

B. Algorithm Flow

According to the principle of the EMD-PCC algorithm, the specific process is shown in Fig. 1.

a. Obtain the phase signal and determine all extreme points.
b. Use a cubic spline curve to fit the envelope sum of the extreme points as $e_{max}(t)$ and $e_{\min}(t)$; then, obtain the average value $(m(t))$ of the envelopes and subtract it from $h(t) = \phi(t) - m(t)$.
c. Determine whether $h(t)$ is IMF according to the preset criteria.
d. If not, replace $\phi(t)$ by $h(t)$ and repeat the above steps until the criterion is satisfied; then, $h(t)$ is $IMF_i(t)$ that must be extracted.

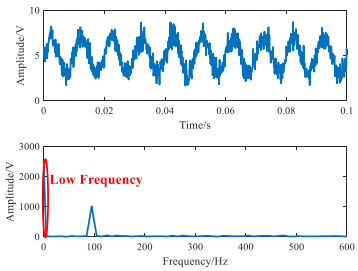

Fig. 2. Simulation signal.

e. If the first-order IMF is obtained, remove it from the original signal and repeat the above steps until the residual component. r_n is only a monotonic sequence or a constant-value sequence. After the EMD method decomposition, the original signal $\phi(t)$ can be decomposed into a series of IMF and residual components. The decomposed signal is shown in Eq. 6.

$$\phi(t) = \sum_{i=0}^{N} IMF_i(t) + r_n(t) \tag{1}$$

where $IMF_i(t)$ is the decomposed modal function, and $r_n(t)$ is the residual component.

f. Calculate the Pearson correlation coefficient (PCC) between $IMF_i(t)$ and $r_n(t)$ obtained by the EMD method. The PCC is defined as Eq. (7).

$$PCC_i = \frac{\sum_{j=1}^{n}(x_j - \overline{x})(y_j - \overline{y})}{\sqrt{[\sum_{j=1}^{n}(x_i - \overline{x})^2][\sum_{j=1}^{n}(y_i - \overline{y})^2]}} \tag{2}$$

where x_j and y_j are two variables of the data; $\overline{x}$ and $\overline{y}$ are the arithmetic means of the data; n is the length of the variable.

g. Define the correlation coefficient: 0.8-1.0 is very strong correlation; 0.6-0.8 is strong correlation; 0.4-0.6 is moderate correlation; 0.2-0.4 is weak correlation; 0.0-0.2 is very weak or no correlation. According to each calculated PCC value, the selected threshold is the correlation coefficient in the range of 0.4-1.0. Linear superposition is performed, and signals outside the threshold are discarded.

C. Algorithm Simulation

In the simulation experiment, the original signal is a sine signal with a frequency of 100 Hz and an amplitude of 1 V. Then, 10 dB white Gaussian noise and a 3 V DC component are added to the original signal. The experimental simulation is shown in Fig. 2. Because the simulated signal is nonlinear and nonstationary, we use the EMD method to decompose the original signal with noise. Six IMFs and 1 RES are obtained. The frequency of the IMF is gradually reduced from high to low. Gaussian white noise and DC components are also superimposed in the IMF. A standard sinusoidal signal cannot be extracted from the original signal. To reduce the effect of noise, we calculate the PCC between the original signal and each IMF and RES, as shown in Fig. 3. According

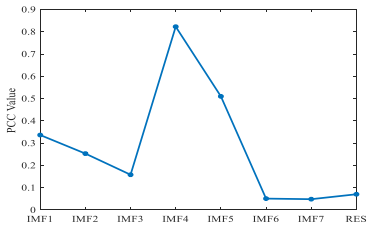

Fig. 3. Correlation coefficient between phase signal and IMF.

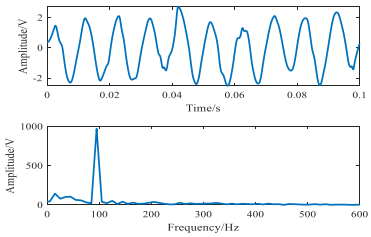

Fig. 4. Time-frequency domain after processing.

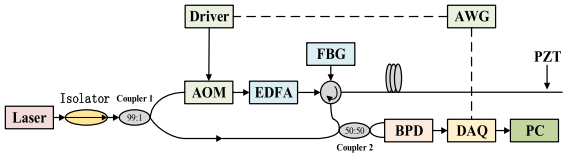

Fig. 5. Φ-OTDR system.

to each calculated PCC value, the selected threshold is the correlation coefficient in the range of 0.4-1.0. After the linear superposition is performed, signals outside the threshold are discarded to obtain the signal, as shown in Fig. 4. We use the signal-noise ratio (SNR) equation to evaluate the effect of noise reduction using Eq. (3). By adopting the EMD-PCC method, the SNR increases from 7.32 dB to 13.68 dB, and the noise suppression effect is better.

$$SNR = 10\lg(Ps/Pn) \tag{3}$$

where P_s is the effective power of the signal. P_n is the effective power of the noise.

III. Experimental Verification

A. Experimental Setup

1) Φ-OTDR System: When the intrusion position on the optical fiber line is disturbed, the elastic-optical effect causes the refractive index of the corresponding position on the optical fiber to change, which makes the optical phase change. Due to the interference of light, the change in phase causes the intensity change of Rayleigh backscattered light. Therefore, the intrusion location is determined by the light intensity. The phase is demodulated to obtain the intrusion disturbance signal. The Φ-OTDR optical system is built, as shown in Fig. 5. The optical system uses a narrow linewidth laser (ECL) to emit light with a wavelength of 1550.12 nm, and its output power is 11.50 mW. The laser produces continuous high-coherent light that passes through the isolator. The continuous light (CW) is divided into two parts by the 3 dB fiber coupler I: 99% signal light and 1% local oscillator light (LO). A 200 MHz optical pulse frequency shift is generated by an acousto-optic modulator (AOM) driven by a waveform generator (AWG). The erbium-doped fiber amplifier (EDFA) amplifies the signal

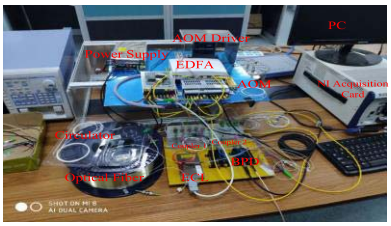

Fig. 6. Experimental platform.

light power. Then, it is fed into the sensing fiber through a 4 port circulator, and the sensing fiber is 10.05 km long. The PZT analog vibration signal is loaded at the 10 km position of the sensing fiber. One port of the circulator is connected to a fiber Bragg grating (FBG). The reflected back Rayleigh scattered light and 1% of the local oscillator light interfere with the 3 dB fiber coupler II with a splitting ratio of 50:50 to generate an optical beat signal. The photoelectric balance detector (BPD) is used to detect the optical beat signal, and its mathematical expression is Eq. (4). A data acquisition card (DAQ) is used to sample discrete samples of the output signal; finally, the signal is processed and displayed by the computer. Fig. 6 shows the platform for the actual experiment.

$$I(t) = 2\alpha E_{LO}(t)E_b(t)\cos(2\pi\,\Delta f t + \phi(t) + \phi_0) \tag{4}$$

where α is the BPD photoelectric conversion coefficient; E_{LO} and E_b are the amplitudes of the local vibration light and signal light, respectively; Δf is the AOM frequency shift; $\phi(t)$ is the phase change caused by the measured vibration signal; and ϕ_0 is the phase change of the light caused by the system environment noise α.

2) I/Q Quadrature Demodulation: According to Eq. (4), the PZT vibration signal is wrapped in the phase. In this paper, I/Q quadrature demodulation is used to obtain the signal. The steps of the I/Q phase demodulation method are as follows:

a. Generate a pair of quadrature digital signals with identical frequency to the heterodyne detection. The mathematical expressions are Eqs. (5) and (6).

$$y_{r1} = C\cos(2\pi\,\Delta f t + \phi_r) \tag{5}$$
$$y_{r2} = C\sin(2\pi\,\Delta f t + \phi_r) \tag{6}$$

where C is the amplitude of a pair of generated quadrature signals, and ϕ_r is the random phase noise.

b. Beat frequency signal $I(t)$ is multiplied by Eqs. (5) and (6). Then, a pair of orthogonal I and Q signals is obtained after low-pass filtering. The mathematical expressions are Eqs. (7) and (8).

$$I = E_s\cos[\phi(t) + \phi_0 - \phi_r] \tag{7}$$
$$Q = -E_s\sin[\phi(t) + \phi_0 - \phi_r] \tag{8}$$

where Es is the amplitude of the obtained pair of orthogonal signals I and Q, and $\phi_0 - \phi_r$ is the phase noise.

c. The I and Q signals are processed by arctangent operation, range expansion and phase unwrapping. The phase change at the adjacent position after the peak of phase difference change is used to demodulate the phase. The processing flow is shown in Fig. 7.

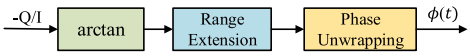

Fig. 7. Phase processing.

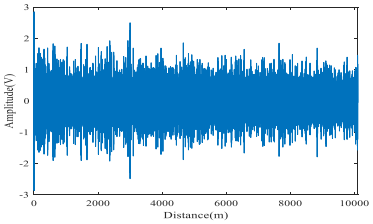

Fig. 8. Beat signal.

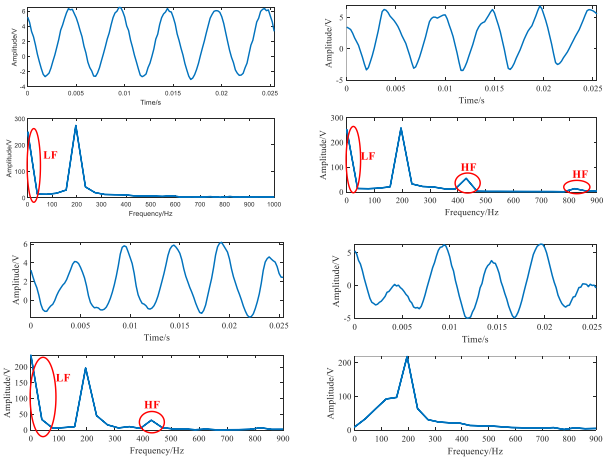

Fig. 9. The frequency of sinusoidal disturbance signal is 200Hz (a) original data (b) wavelet denoising (c) EMD-soft denoising (d) EMD-0PCC denoising.

B. Experimental Results and Analysis

In this experiment, PZT is used as the vibration source, and the driving signal is provided by the signal generator. The PZT drive signal is a sine wave with a frequency of 500 Hz and an amplitude of 500 mV, which is placed at 10 km on the optical fiber. According to the experiment in Fig. 7, the beat signal is shown in Fig. 8. Theoretically, the beat frequency signal is a standard sine signal. However, due to the attenuation of Rayleigh backscattered light and interference fading, the beat frequency signal is not a standard sinusoidal signal. Among them, the sources of phase noise mainly include: a. a frequency drift of laser; b. polarization fading noise; c. coherent fading noise; d. effect of the extinction ratio of acousto-optic modulator (AOM); e. shot noise and so on.

The beat signal in Fig. 8 applies the I/Q quadrature demodulation algorithm to demodulate the phase signal, i.e., the external disturbance signal. In this paper, the PZT simulation disturbance signal frequencies are 200 Hz, 300 Hz, 400 Hz, and 500 Hz for 4 groups of intrusion disturbance experiments, and the experimental results are shown in Figs. 9(a)-12(a). The experimental results show a low-frequency component in the demodulated disturbance signal, which affects the demodulation result. We use LF to represent low-frequency components and HF to represent high-frequency components. To filter out the low-frequency components, correctly demodulate the disturbance signal and reduce the noise interference, we denoise the demodulated disturbance signal. In this paper, wavelet denoising, EMD-soft denoising and EMD-PCC denoising

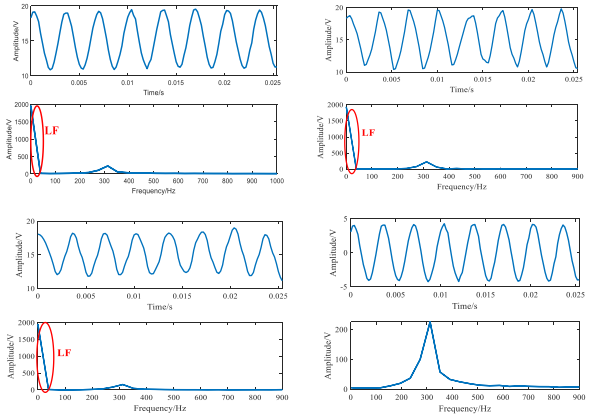

Fig. 10. The frequency of sinusoidal disturbance signal is 300Hz (a) original data (b) wavelet denoising (c) EMD-soft denoising (d) EMD-PCC denoising.

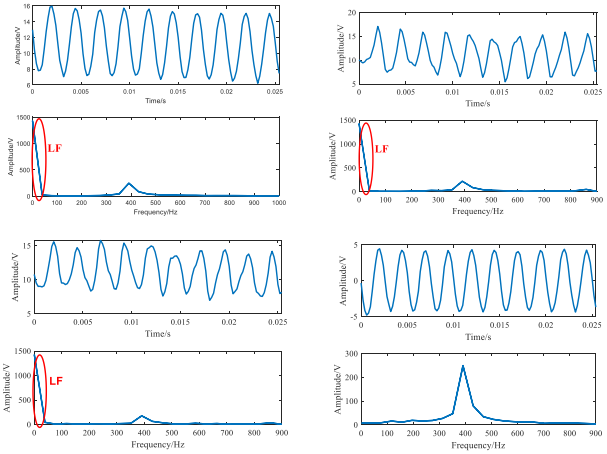

Fig. 11. The frequency of sinusoidal disturbance signal is 400Hz (a) original data (b) wavelet denoising (c) EMD-soft denoising (d) EMD-PCC denoising.

methods are compared and analyzed. The experimental results show that after wavelet denoising, the demodulated disturbance signal has distortion, and there are low- frequency or high-frequency components, as shown in Figs. 9(b)-12(b). Similarly, after the EMD-soft denoising for the demodulated disturbance signal, the signal appears distorted and has low-frequency or high-frequency components, as shown in Figs. 9(c)-12(c). However, the demodulated disturbance signal is not distorted, and the low-frequency components are filtered out using the EMD-PCC denoising method. Only 200 Hz, 300 Hz, 400 Hz or 500 Hz are dominant in the demodulated signal, as shown in Figs. 9(d)-12(d). Therefore, the proposed method is better than the other two denoising methods and can more accurately demodulate the disturbance signal.

This paper further verifies the applicability of the EMD-PCC denoising method when the disturbance signal is a sawtooth signal, and the frequencies are 400 Hz and 500 Hz. The demodulated disturbance signal is shown in Figs. 13 (a) and 14 (a). There is a low-frequency component in the disturbance signal before denoising, which affects the accuracy of the demodulated signal. In this paper, the demodulated disturbance signal is denoised by EMD-PCC, and the low-frequency component can be filtered out. Only the 400-Hz and 500-Hz sawtooth signals are dominant, as shown

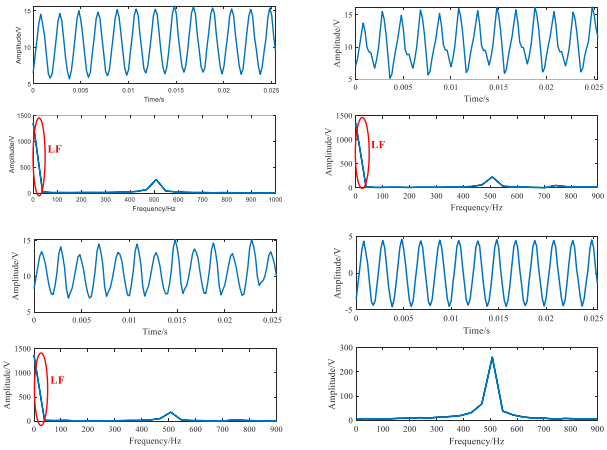

Fig. 12. The frequency of sinusoidal disturbance signal is 500Hz (a) original data (b) wavelet denoising (c) EMD-soft denoising (d) EMD-PCC denoising.

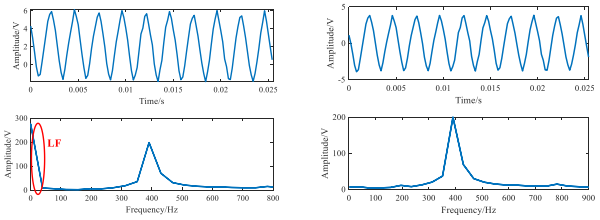

Fig. 13. The frequency of sawtooth disturbance signal is 400Hz (a) original data (b) EMD-PCC denoising.

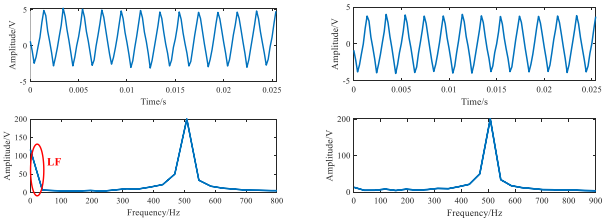

Fig. 14. The frequency of sawtooth disturbance signal is 500Hz (a) original data (b) EMD-PCC denoising.

in Figs. 13(b) and 14 (b). Therefore, the EMD-PCC denoising method is also applicable to the case in which the disturbance signal is a sawtooth signal. Similarly, this method can be applied to signal models with arbitrary disturbance signals.

IV. Conclusion

A new method based on empirical mode decomposition and Pearson correlation coefficient fusion (EMD-PCC) is proposed to suppress the phase noise demodulated by the Φ-OTDR system. In this paper, simulation experiments are performed for the proposed EMD-PCC method. The experimental results show that the SNR increases from 7.32 dB to 13.68 dB. Then, the Φ-OTDR system is built to verify the effectiveness of the algorithm. The specific method is as follows: first, load the PZT at 10 km of the sensing fiber to collect the beat signal detected by the optical system; second, process the beat signal through related mathematical processing and I/Q quadrature demodulation to demodulate the phase signal; finally, decompose the phase signal using EMD to obtain the IMF and RES. The Pearson correlation coefficient with the phase signal is calculated; 0.4-1.0 is selected as the threshold interval, and the filtered IMF and RES are superimposed. In this paper,

the experimental verification is performed for PZT analog disturbance signal frequencies of 200 Hz, 300 Hz, 400 Hz and 500 Hz. Then, wavelet denoising and EMD-soft denoising are compared with EMD-PCC denoising. Experimental results show that the proposed method can accurately restore the disturbance signal. The experiment of sawtooth disturbance signal frequencies of 400 Hz and 500 Hz verifies the applicability of the algorithm. Experimental results show that the method is suitable for other arbitrary forms of disturbance signals.

REFERENCES

[1] T. Yamate, G. Fujisawa, and T. Ikegami, "Optical sensors for the exploration of oil and gas," *J. Lightw. Technol.*, vol. 35, no. 16, pp. 3538–3545, Aug. 15, 2017, doi: 10.1109/JLT.2016.2614544.

[2] F. Poletto, D. Finfer, P. Corubolo, and B. Farina, "Dual wavefields from distributed acoustic sensing measurements," *Geophysics*, vol. 81, no. 6, pp. D585–D597, Nov. 2016, doi: 10.1190/geo2016-0073.1.

[3] S. Xie, Q. Zou, L. Wang, M. Zhang, Y. Li, and Y. Liao, "Positioning error prediction theory for dual Mach–Zehnder interferometric vibration sensor," *J. Lightw. Technol.*, vol. 29, no. 3, pp. 362–368, Feb. 2011, doi: 10.1109/jlt.2010.2102339.

[4] C. Pan, X. R. Liu, H. Zhu, X. K. Shan, and X. H. Sun, "Distributed optical fiber vibration sensor based on Sagnac interference in conjunction with OTDR," *Opt. Express*, vol. 25, no. 17, pp. 20056–20070, Aug. 2017, doi: .10.1364/OE.25.020056.

[5] Y. Mao *et al.*, "Simultaneous distributed acoustic and temperature sensing using a multimode fiber," *IEEE J. Sel. Topics Quantum Electron.*, vol. 26, no. 4, Jul. 2020, Art. no. 5600207, doi: 10.1109/jstqe.2020.2964398.

[6] A. Barrias, J. Casas, and S. Villalba, "A review of distributed optical fiber sensors for civil engineering applications," *Sensors*, vol. 16, no. 5, p. 748, May 2016, doi: 10.3390/s16050748.

[7] A. G. Leal *et al.*, "Quasi-distributed torque and displacement sensing on a series elastic actuator's spring using FBG arrays inscribed in CYTOP fibers," *IEEE. Sensors J*, vol. 19, no. 11, pp. 4051–4061, Jun. 2019, doi: .10.1109/JSEN.2019.2898722.

[8] A. G. Leal-Junior, C. R. Díaz, C. Marques, M. J. Pontes, and A. Frizera, "Multiplexing technique for quasi-distributed sensors arrays in polymer optical fiber intensity variation-based sensors," *Opt. Laser Technol.*, vol. 111, pp. 81–88, Apr. 2019, doi: 10.1016/j.optlastec.2018.09.044.

[9] Y. Lu, T. Zhu, L. Chen, and X. Bao, "Distributed vibration sensor based on coherent detection of phase-OTDR," *J. Lightw. Technol.*, vol. 15, pp. 3243–3249, Nov. 2010, doi: 10.1109/jlt.2010.2078798.

[10] Z. Qin, T. Zhu, L. Chen, and X. Bao, "High sensitivity distributed vibration sensor based on polarization-maintaining configurations of phase-OTDR," *IEEE Photon. Technol. Lett.*, vol. 23, no. 15, pp. 1091–1093, Aug. 2011, doi: 10.1109/lpt.2011.2157337.

[11] T. Zhu, Q. He, X. Xiao, and X. Bao, "Modulated pulses based distributed vibration sensing with high frequency response and spatial resolution," *Opt. Express*, vol. 21, no. 3, pp. 2953–2963, Feb. 2013.

[12] A. Masoudi, M. Belal, and T. P. Newson, "A distributed optical fibre dynamic strain sensor based on phase-OTDR," *Meas. Sci. Technol.*, vol. 24, no. 8, Aug. 2013, Art. no. 085204, doi: 10.1088/0957-0233/24/8/085204.

[13] A. Masoudi, M. Belal, and T. P. Newson, "Distributed dynamic large strain optical fiber sensor based on the detection of spontaneous Brillouin scattering," *Opt. Lett.*, vol. 38, no. 17, pp. 3312–3315, Sep. 2013, doi: 10.1364/OL.38.003312.

[14] G. Fang, T. Xu, S. Feng, and F. Li, "Phase-sensitive optical time domain reflectometer based on phase-generated carrier algorithm," *J. Lightw. Technol.*, vol. 33, no. 13, pp. 2811–2816, Jul. 1, 2015, doi: 10.1109/jlt.2015.2414416.

[15] Y. Lv *et al.*, "Eliminating phase drift for distributed optical fiber acoustic sensing system with empirical mode decomposition," *Sensors*, vol. 19, no. 24, p. 5392, Dec. 2019, doi: 10.3390/s19245392.

[16] Z. Qin, L. Chen, and X. Bao, "Continuous wavelet transform for non-stationary vibration detection with phase-OTDR," *Opt. Express*, vol. 20, no. 18, pp. 20459–20465, 2012, doi: 10.1364/OE.20.020459.

[17] Z. Qin, L. Chen, and X. Bao, "Wavelet denoising method for improving detection performance of distributed vibration sensor," *IEEE Photon. Technol. Lett.*, vol. 24, no. 7, pp. 542–544, Apr. 2012, doi: 10.1109/lpt.2011.2182643.

[18] H. Wu, S. Xiao, X. Li, Z. Wang, J. Xu, and Y. Rao, "Separation and determination of the disturbing signals in phase-sensitive optical time domain reflectometry (Phi-OTDR)," *J. Lightw. Technol.*, vol. 33, no. 15, pp. 3156–3162, Aug. 1, 2015, doi: 10.1109/jlt.2015.2421953.

[19] H. He *et al.*, "SNR enhancement in phase-sensitive OTDR with adaptive 2-D bilateral filtering algorithm," *IEEE Photon. J.*, vol. 9, no. 3, Jun. 2017, Art. no. 6802610, doi: 10.1109/jphot.2017.2700894.

[20] F. Liu, G. Hu, C. Chen, W. Chen, and C. Song, "Significant dynamic range and precision improvements for FMF mode-coupling measurements by utilizing adaptive wavelet threshold denoising," *Opt. Commun.*, vol. 426, pp. 287–294, Nov. 2018, doi: 10.1016/j.optcom.2018.05.053.

[21] S. Qu *et al.*, "Phase sensitive optical time domain reflectometry based on compressive sensing," *J. Lightw. Technol.*, vol. 37, no. 23, pp. 5766–5772, Dec. 1, 2019, doi: 10.1109/jlt.2019.2938789.

[22] S. Qu, J. Chang, Z. Cong, H. Chen, and Z. Qin, "Data compression and SNR enhancement with compressive sensing method in phase-sensitive OTDR," *Opt. Commun.*, vol. 433, pp. 97–103, Feb. 2019, doi: 10.1016/j.optcom.2018.09.064.

[23] L. Du, B. Wang, Y. Li, and H. Liu, "Robust classification scheme for airplane targets with low resolution radar based on EMD-CLEAN feature extraction method," *IEEE Sensors J.*, vol. 13, no. 12, pp. 4648–4662, Dec. 2013, doi: 10.1109/jsen.2013.2272119.

[24] S. Maurya, V. Singh, and N. K. Verma, "Condition monitoring of machines using fused features from EMD-based local energy with DNN," *IEEE Sensors J.*, vol. 20, no. 15, pp. 8316–8327, Aug. 2020, doi: 10.1109/jsen.2019.2927754.

[25] O. A. Omitaomu, V. A. Protopopescu, and A. R. Ganguly, "Empirical mode decomposition technique with conditional mutual information for denoising operational sensor data," *IEEE Sensors J.*, vol. 11, no. 10, pp. 2565–2575, Oct. 2011, doi: 10.1109/jsen.2011.2142302.

[26] M. He, L. Feng, and J. Qu, "Denoising algorithm of OTDR signal based on clear iterative EMD interval-thresholding," *Opt. Commun.*, vol. 453, Dec. 2019, Art. no. 124352, doi: 10.1016/j.optcom.2019.124352.

[27] M. Li, X. Xiong, Y. Zhao, and Y. Ma, "Denoising method based upon ECEMD and selective addition for phi-OTDR," *Opt. Commun.*, vol. 452, pp. 313–320, Dec. 2019, doi: 10.1016/j.optcom.2019.07.053.

Wei Chen is currently pursuing the Ph.D. degree with the School of Opto-Electronic Engineering, Changchun University of Science and Technology. As an Assistant Research Fellow, he also works with the Changchun Institute of Optics, Fine Mechanics and Physics, Chinese Academy of Sciences. His main research interests include optical imaging and detection and recognition of cross-medium target.

Xiaohui Ma is a Research Fellow with the State Key Laboratory of High Power Semiconductor Laser and the School of Opto-Electronic Engineering, Changchun University of Science and Technology. His main research interests include high power semiconductor laser device technology and fiber coupling technology.

Qinglin Ma is currently pursuing the master's degree with the School of Opto-Electronic Engineering, Changchun University of Science and Technology. His main research interest includes photoelectric signal demodulation and processing.

Jiajie Wen is currently pursuing the master's degree with the School of Opto-Electronic Engineering, Changchun University of Science and Technology. His main research interest includes photoelectric signal demodulation and processing.